Journal of Materials Chemistry A

Accepted Manuscript

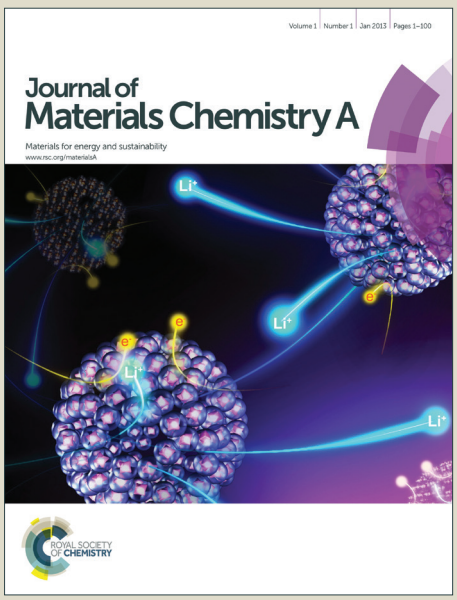

ROYAL SOCIETY OF CHEMISTRY

www.rsc.org/materialsA

Journal Name

ARTICLE

Nontoxic Solvent Based Sol-Gel Cu_2ZnSnS_4 Thin Film for High Efficiency and Scalable Low-cost Photovoltaic Cells

Received 00th January 20xx,
Accepted 00th January 20xx

DOI: 10.1039/x0xx00000x

www.rsc.org/

Venkatesh Tunuguntla[a,b,c,d], Wei-Chao Chen[a,c,f], Pei-Hsuan Shih[e], Indrajit Shown[a], Yi-Rung Lin[a,c,g], Jih-Shang Hwang[e], Chih-Hao Lee[f], Li-Chyong Chen[c*] and Kuei-Hsien Chen[a,c*]

Non-toxic sol-gel spin coating approach is one of the attractive routes to achieve high atom economy, good quality Cu_2ZnSnS_4 (CZTS) thin film. In this paper, we introduce 1,3-dimethyl-2-Imadazolidinone as a solvent for the preparation of highly viscos, homogeneous, nontoxic CZTS ink that eliminates the need for use of additional binders or additives to disperse the precursors. In addition, we further report that annealing the spin coated CZTS thin film in 6% diluted H_2S gas with externally supplied tin and sulfur environment to suppress the loss of tin from the thin-film surface and to enhance the device performance. CZTS grain sizes of greater than 0.7μm have been achieved with no detectable presence of carbon rich layer or layers containing fine grain sizes at the Mo/CZTS interface. An efficiency of 5.67% for the champion device fabricated here has been achieved with an open circuit voltage of 0.58 V, short current density of 18.48 mA/cm^2, and a fill factor of 53.14%.

Introduction

In recent years, $Cu_2In_xGa_{1-x}Se_2$ (CIGS) and CdTe solar cells have significantly improved their cell and module efficiencies but the scarcity of indium and gallium, toxicity of cadmium may restrict the production capacity for a growing multi TW energy demand in long run.[1] In order to reduce the material cost, replacement of these expensive and toxic metals is considered to be a promising approach towards future low-cost thin film based solar cell.[2] For these reasons, kesterite semiconductors Cu_2ZnSnS_4 (CZTS), $Cu_2ZnSnSe_4$ (CZTSe) and $Cu_2ZnSn(S_xSe_{(1-x)})_4$ (CZTSSe) offer an alternative to CIGS and CdTe technology. Due to the combined advantage of S and Se, in terms of tunability of the band gap (E_g) and high conductivity, CZTSSe solar cell are highly attractive for achieving high-performance compared to either CZTS or CZTSe. However, the observed V_{OC} deficit in CZTSSe solar cells is due to the band gap fluctuations and electrostatic potential fluctuations in the absorber material (pentenary compound), which potentially limiting further improvements in CZTSSe solar cell efficiency.[3] On the other hand, the V_{OC} deficit of CZTSSe solar cell[4] (**513 vs. 820 mV**, Eg= 1.13 eV) is quite comparable to the V_{OC} deficit of CZTS solar cell[5] (**708 vs. 1100 mV**, Eg= 1.5 eV). Since CZTS is a relatively less complex system (quaternary compound) and for long term goal to achieve > 20% efficiency, CZTS is a more promising material for low cost and high efficiency solar cells with large open circuit voltage. It is, therefore, necessary to develop novel and environmentally friendly synthesis processes for high quality CZTS thin-film growth and to obtain better understanding of the annealing conditions of CZTS grain growth for achieving high efficiency solar cells.

IBM has reported a device with 12.7% efficiency[6,7] fabricated with CZTSSe absorber layer deposited by spin-coating process using a hydrazine-based ink. However, hydrazine is extremely toxic, flammable, highly reactive and explosive in nature, which limits the use of this solvent for large-scale applications. Due to these concerns over the solvent properties, a number of researchers have made effort to develop other non-toxic solvents to synthesize the kesterite absorber layer, but the reported efficiencies are relatively low compared to the hydrazine process. In 2012, Woo *et al.* demonstrated the fabrication of CZTS solar cell with an efficiency of 5.1% using ethanol as a solvent.[8] This is the highest reported efficiency for a non-toxic sol-gel spin coating approach so far. In general, alcohol-based solvents have low boiling point, like hydrazine, which is advantageous since they lead to reduce the carbon residue from the solvent after annealing the spin coated thin film. However, the polarity of the alcohol based solvents is very low compared to hydrazine,

[a] Institute of Atomic and Molecular Sciences, Academia Sinica, Taipei, Taiwan
[b] Department of Chemistry, National Tsing Hua University, Hsinchu, Taiwan
[c] Center for Condensed Matter Sciences, National Taiwan University, Taipei, Taiwan
[d] Molecular Science and Technology (MST) Program, Taiwan International Graduate Program (TIGP), Academia Sinica, Taipei, Taiwan
[e] Institute of Optoeletronic science, National Taiwan Ocean University, 2 Pei-Ning Road, Keelung, Taiwan
[f] Engineering and System Science, National Tsing Hua University, No. 101, Section 2, Kuang-Fu Road, Hsinchu, Taiwan
[g] Department of Chemistry, National Taiwan University, No. 1, Sec. 4, Roosevelt Road, Taipei, Taiwan
* E-mail: chenlc@ntu.edu.tw
* E-mail: chenkh@pub.iams.sinica.edu.tw
Electronic Supplementary Information (ESI) available: SEM pictures for CZTS film under different H_2S concentrations, XRD and Raman spectra for CZTS film annealed in 6% H_2S, absorption spectra for pristine and annealed CZTS films, detailed description of solar cell device fabrication. See DOI: 10.1039/x0xx00000x

which makes it challenging to dissolve the precursors in order to achieve highly viscous and homogeneous sol-gel ink. In order to increase the solubility of the precursors and viscosity of the ink, organic binders[9] or stabilizers[10] or toxic complexing agents[11] are generally added to the solvent. These organic stabilizers or binder yield a good homogenous mixture as well as impart optimal viscosity to the precursor ink but these additives invariably leave a carbon rich layer due to carbon residue[12,13] or lead to a formation of small grains[14] at the CZTS/Mo interface after annealing. It has been found that such carbon rich interface has detrimental effects on the device and reduces the performance. Therefore, it is necessary to develop a new high-viscosity sol-gel ink free of binder, stabilizer or complexing agent by using a non-toxic, highly polar solvent alternative to toxic hydrazine.

In this study, we have introduced 1,3-dimethyl-2-Imadazolidinone (DMI) as a solvent for the preparation of high viscosity homogeneous sol-gel CZTS ink without any additional complexing agents. In the method presented here, the crystallinity of the CZTS thin film was improved by annealing in diluted H_2S gas in externally supplied tin and sulfur environment. The significance of the influence of H_2S concentration, annealing temperature, and the effects of tin and sulfur during annealing on CZTS grain growth will be reported in the following.

Experimental

Materials

$Cu(CH_3COO)_2.H_2O$ (98%) from Acros; $ZnCl_2$ (anhydrous 99.999%) from Sigma Aldrich; $SnCl_2$ (anhydrous, 98%) from Acros; thiourea (>99%) from Acros; DMI (≥99.5%) from Fluka; All reagents were used as received from the commercial sources.

Synthesis of CZTS ink

The CZTS ink was prepared by dissolving 8.5 mmol of $Cu(CH_3COO)_2.H_2O$, 6.3 mmol of $ZnCl_2$, 6 mmol of $SnCl_2$ and 26.4 mmol of thiourea into 6.6 mL of 1,3-dimethyl-2-Imadazolidinone (DMI) solvent to yield a 0.64 M solution, and the vial was sealed in a N_2 filled glove box. The solution was then sonicated for 3 hours at room temperature to obtain a homogeneous solution. The solution thus prepared was found to be stable for several weeks, and no precipitates or obvious changes were observed in the ink.

Synthesis of CZTS thin film

The CZTS precursor ink was spin coated on SLG (soda lime glass)/Mo substrate at 3400 rpm for 1 min followed by heat treatment on a hot plate at a temperature of 425°C for 1 min. This was repeated six times to obtain a thick CZTS film (hereafter referred to as pristine film). After the preparation of CZTS pristine film, it was annealed in H_2S environment by tube furnace at 610°C for 8 min in the presence of externally supplied 130 mg of tin pellets and 320 mg of sulfur flakes (the temperature profile is shown in the supporting information, Fig.S5) to yield the desired crystalline CZTS. The concentration of H_2S was controlled by the flow rates of H_2S (10% in N_2) and N_2 gases. Optimization of each parameter was carried out to thoroughly understand the properties of CZTS at high temperatures.

Device fabrication

Finally, the CZTS thin film was used to fabricate a solar-cell device with the following structure: SLG/Mo (900 nm)/CZTS (1.5±0.1 µm)/CdS (50 nm)/ZnO (40 nm)/ITO (350 nm)/Ag. Details of the solar cell device fabrication are provided in the supporting information. After the device fabrication, it was mechanically scribed with a knife to obtain a total device area of 0.15 cm^2.

Characterization

The X-ray diffraction (XRD) measurements were carried out using Bruker D8 Discover X-ray diffractometer with Cu Kα radiation. Raman spectra were recorded on a HORIBA Jobin-YvonLabRAM H800 at 633 nm excitation wavelength. The optical absorption spectra were obtained using JASCO V670 UV-visible-near-infrared spectrophotometer. Scanning electron microscope (SEM, JEOL 6700F), energy dispersive spectroscopy (EDS) and transmission electron microscopy (TEM, JEOL JEM-2100) were used to characterize the surface morphology and elemental composition of CZTS thin films.

Results and discussion

DMI solvent enables complete and uniform dissolution of the precursor and also enables to form CZTS compound at relatively low temperatures without leaving any carbon residue and/or other secondary phase impurities. The obtained homogeneous sol-gel CZTS ink (viscosity is 232 cP at 25°C), as shown in the inset of fig.1, was spin coated on a SLG/Mo substrate (hereafter referred to as pristine film). To investigate the decomposition profile and the formation of CZTS, we performed a Thermo Gravimetric Analysis (TGA) of the precursor ink under N_2 environment. The TGA spectrum, as presented in fig.1, shows a sharp 80% weight loss from 150°C to 300°C due to thermal decomposition of the metal precursor complexes and volatile organic moieties. At 300°C, the formation of CZTS compound is completed, and consequently

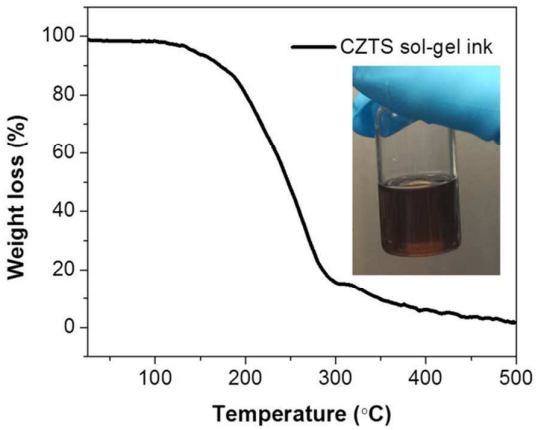

Fig.1 Results of Thermo Gravimetric Analysis (TGA) of CZTS precursor ink in N_2 environment. Inset shows a homogeneous CZTS ink prepared.

the weight loss rate reduces thereafter. The weight loss still continues at a lower rate to beyond 300°C which may be due to the volatile moieties such as SnS desorption, decomposition of residual precursor, excess solvent etc. It is also noteworthy that the TGA spectrum obtained in this work is quite similar to those reported for sol-gel inks prepared using low boiling point (b.p) alcohol[8,15,16] based solvents (typically, b.p of lower than 100°C). Despite the high b.p (225°C) the present DMI solvent, the formation of CZTS compound is observed to take place at a relatively low temperature of 300°C, similar to that with alcohol based solvents. Based on the TGA analysis, we estimate that the hot plate temperature required to remove the solvent and other volatile moieties from the precursor ink during the spin coating must be above 300°C for CZTS formation.

Fig.2(a-f) presents the cross-sectional SEM images and surface morphologies of the pristine and CZTS thin film under different annealing conditions. The spin coated CZTS thin-film with a thickness of 1.9 ± 0.1 µm was obtained after six repeated coatings, as determined from the cross-section SEM image shown in fig.2a. In fig.2d, the top view of the pristine film shows presence of cracks on the surface of spin coated film which occur due to the evaporation of solvent and other volatile organic moieties. Highly crystalline CZTS thin film was achieved by annealing the pristine thin film in reactive gas (H_2S) environment at elevated temperature. The annealing temperature of 610°C used in this work is much higher than the temperature generally used for the conventional annealing process. It is found that the optimum annealing temperature is dependent on the thickness and density of the pristine film, i.e. it is indirectly related to the concentration of the sol-gel ink. It has been observed that high concentration sol-gel ink yields a highly condensed film as compared to the one prepared with low concentration sol-gel ink. The optimum annealing temperature was found to be 610°C for a film thickness of 1.9 ± 0.1 µm prepared using a solution of 0.64M concentration.

The charge collection under AM 1.5 illumination is known to depend on the vertical grain size of the CZTS thin film, since the electrons tend to recombine at the grain boundaries because of the high surface potentials at grain boundaries compared to grain interiors.[17] According to the literature, the concentration of H_2S during the annealing process plays an important role in the formation of larger grain size.[18,19] It is also well known that the H_2S concentration required during the annealing process may vary depending on the annealing conditions, such as time, temperature, thickness of the film and type of the precursor film (for example, metal stacking film or small-grained film or alloyed film, etc.). The formation and gradual increase in CZTS grain size was achieved with optimization of H_2S concentration during annealing. The effect of H_2S concentration on the size and formation of grains was observed from the SEM images as shown in fig.S1(a-e) of the supporting information. Here, the concentration of H_2S was controlled by controlling the flow rates of H_2S (10% in N_2) and N_2 gases. At 6% of H_2S concentration, the pristine film completely converted into a large grain CZTS film with good crystallinity as shown in fig.S1(e).

Apart from the annealing temperature, annealing time is also an important parameter due to the reactivity of molybdenum substrate with CZTS. During annealing, S^{2-} from H_2S or from CZTS reacts with molybdenum substrate, resulting in formation of an interfacial MoS_x layer at the Mo/CZTS interface.[20] This MoS_x layer possesses a high series resistance and acts as an electron sink resulting in device with low fill factor due to the carrier recombination.[21] It has been reported that shorter annealing time (3 min) is sufficient to achieve good quality CZTS thin film. However, only few groups have

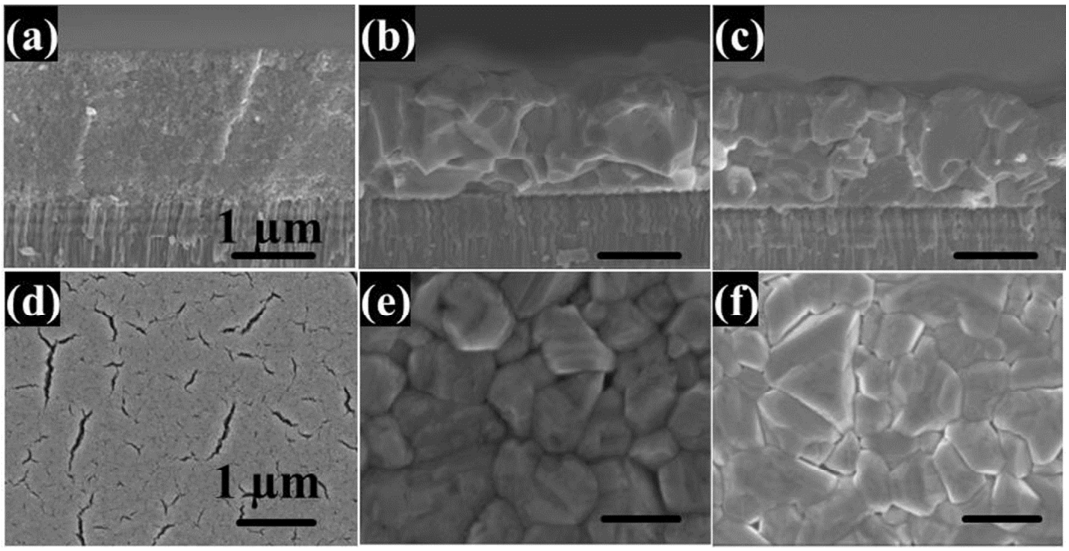

Fig.2 a) Cross-sectional SEM image of the pristine CZTS thin film after six spin coatings, b) and c) cross-sectional SEM images of annealed CZTS thin films without and with externally supplied Sn and S in 6% diluted H_2S environment, respectively, d) Top view SEM image of pristine CZTS thin film, e) and f) Top view SEM images of annealed CZTS thin films without and with externally supplied Sn and S annealed in 6% of diluted H_2S environment, respectively.

reported achieving a good quality of CZTS thin film with high solar cell efficiency at annealing time of less than 10 min.[22-24] In order to reduce the thickness of MoS_x layer at the interface, we annealed our pristine thin film for 8 min under optimized conditions. In fig.2b, the cross-section SEM image of annealed CZTS thin film shows that the vertical grain size is greater than 0.7 µm without presence of any carbon rich layer or small grains at the Mo/CZTS interface.[25,26] The thickness of the final annealed film is reduced to 1.5±0.15µm, due to the volatility of residual solvent and other moieties in the pristine thin film. From the top view of SEM picture shown in fig.2e, it can be seen that the surface of annealed CZTS thin film is quite smooth without any detrimental pores.

It is well known that under vacuum, CZTS tends to decompose into Cu_2S, ZnS, SnS_2 and desorbs SnS and S_2 as gaseous products from the thin film surface at temperature greater than 350°C.[27] There exists equilibrium between the decomposed binary phases (Cu_2S, ZnS, SnS_2) at the surface, desorbed gaseous products (SnS, S_2) and CZTS.[28] It has been reported that the decomposition rate increases at elevated temperatures and leads to formation of large amounts of low band gap (< 1.5 eV) impurities such as Cu_2SnS_3, SnS, $Cu_{2-x}S$, SnS_2 etc. These low band gap impurities are detrimental to the device performance since their band gap lies within the bandgap of absorber layer and act as recombination centers. Particularly, the loss of tin is strongly affected by the extended annealing time and high temperature, which suggests that a shorter annealing time is desirable at elevated temperatures. We further optimized the annealing process with externally supplied Sn (130 mg) and sulfur (320 mg) under 6% H_2S gas environment at 610°C for 8 min in tube furnace (here after this process referred as "modified annealing", see fig.S5 of the supporting information). The short annealing time not only reduces the formation of thick MoS_x layer at Mo/CZTS interface but also decreases desorption of volatile gases from the CZTS surface. The SEM images, shown in fig.2c and 2f, of modified annealed CZTS film, do not appear very different from those obtained from "H_2S only" annealed film shown in fig.2b and 2e. However, no severe detrimental effect on either the morphology of CZTS or Mo/CZTS interface are observed due to the enhanced reactivity of the in-situ formed SnS vapor during the modified annealing process.

The crystal structure, phase formation and quality of the pristine CZTS thin film annealed under H_2S environment with externally supplied Sn and S environment were characterized by XRD and Raman analyses, as shown in fig.3. The XRD spectrum of pristine CZTS thin film shown in fig.3a displays peaks at 28.5°, 47.3° and 56.1°, which represent the characteristic diffraction of (112), (220) and (312) planes, respectively, of the kesterite structure of Cu_2ZnSnS_4 (JCPDS no.26-0575). Broadening of the XRD peaks indicates polycrystalline nature of CZTS nanocrystals in the pristine thin film. The XRD pattern of the CZTS thin film obtained after modified annealing under H_2S environment are shown in fig.3b.The observed diffraction pattern matches very well with that of the standard tetragonal Cu_2ZnSnS_4 pattern. The narrow widths of the XRD peaks indicate greatly improved crystallinity

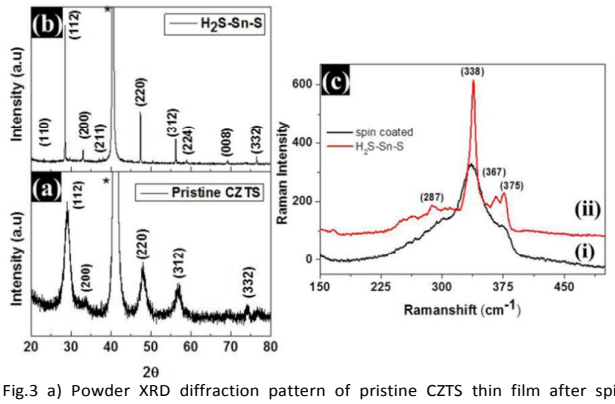

Fig.3 a) Powder XRD diffraction pattern of pristine CZTS thin film after spin coating on Mo substrate b) Powder XRD diffraction pattern of CZTS thin film on Mo substrate annealed in 6% of H_2S environment with externally supplied Sn and sulfur environment. (Mo peaks are labelled with *) c)Raman spectrum recorded with 633 nm excitation wavelength i) spin coated CZTS thin film ii) CZTS thin film on Mo substrate annealed in 6% H_2S environment with externally supplied Sn and sulfur environment.

of CZTS. From the XRD and Raman analysis both H_2S (fig.S3) and Sn-S-H_2S thin films show similar patterns and we haven't identified any major segregation of secondary phases. Usually, the narrow thermodynamic stability region of CZTS causes precipitation of excessive elements in form of secondary phases under non-stoichiometric conditions. Never the less, in the present study, we have optimized the composition of the absorber layer by using copper-poor, zinc-rich conditions with an expectation that formation of trace amounts of ZnS as a competing phase in the final CZTS thin film. Cubic ZnS as well as cubic Cu_2SnS_3 display diffraction patterns identical to tetragonal CZTS, and these are also the possible secondary phases that may exist along with CZTS after annealing. In order to observe and distinguish the presence of secondary phases in CZTS, Raman spectroscopy analysis is applied. The Raman spectra presented in fig.3c were recorded with 633 nm excitation wavelength, which show that the pristine thin film exhibits a strong and broad peak at 338 cm^{-1} corresponding to the CZTS A1 mode. The observed broadening of Raman peak is attributed to phonon confinement within the CZTS nanocrystals. The Raman spectrum of CZTS thin film annealed using the modified process shows the sharp CZTS characteristics peaks without additional impurity peaks. Thus, from the XRD and Raman analyses, it is clearly observed that no serious segregation of secondary phases has occurred in the modified annealed thin film.

The composition of H_2S annealed and modified annealed absorber layers of CZTS films were estimated from the EDS measurement. From the top view, the final composition of H_2S annealed CZTS film was determined to be $Cu_{2.04\pm0.04}Zn_{1.31\pm0.01}SnS_{3.43\pm0.03}$ after averaging at five random locations. However, the EDS only reveal the data of several nanometers of the top surface due to the limited penetration ability of an electron probe. To avoid this limitation, we also measured the cross-sectional depth profile of the composition in the H_2S annealed CZTS thin film, which is shown in the fig.S3 of supporting information. The depth profile shows non homo-

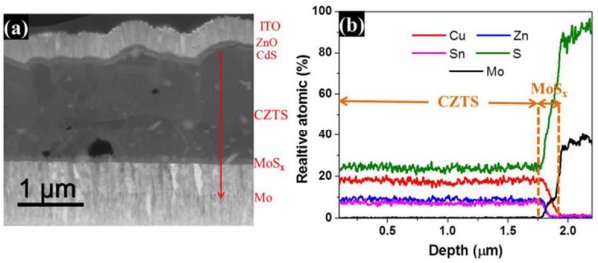

Fig.4 a) Dark field scanning transmission electron microscopy (STEM) image of 5.67% champion CZTS solar cell. Inset shows the direction and position of EDS line scan. b) Cross-section depth profile of CZTS annealed in H_2S with externally provided Sn and sulfur environment.

geneous distribution of elemental composition, especially at the surface of the film. It is clearly observed that loss of Sn from the CZTS surface is extremely serious at the elevated temperature, due to the previously mentioned SnS and S_2 desorption from the CZTS film, leaving a high Zn/Sn ratio at the surface. According to the literature, a minimum amount of S_2 and SnS partial pressures are required at any particular temperature for the backward reaction of this reversible process to occur.[28] In the present experiments, this was achieved successfully by annealing the pristine CZTS thin film in externally provided tin metal (Sn) and sulfur (S). Enhancement in the final efficiency of the device has been reported in the literature with Sn and S assisted annealing, although proper experimental evidence is lacking for SnS desorption from the film surface.[29]

To investigate the effect of modified annealing on the composition of CZTS film, an EDS line scan was performed on a single CZTS grain so as to avoid the fluctuations in elemental composition that generally occur at grain boundaries. The arrow mark, as shown in fig.4a, shows the direction and position of the EDS line scan that covers the entire thickness of the device from film surface to molybdenum back contact. The cross sectional depth profile, thus obtained, is shown in fig.4b, which shows highly homogeneous elemental composition throughout the absorber layer, which we believe has been achieved by successfully reducing SnS desorption from the film surface. This suggests that modified annealing, especially if the annealing temperature is above 550°C, must be performed to suppress the desorption of SnS and S_2 gasses and to achieve homogeneous elemental composition throughout the film thickness (in contrast to in-homogenous H_2S only annealed case CZTS film shown in fig.S3. Dark field scanning transmission electron microscopy (STEM) image of the champion device is shown in fig.4a. The observed pores at the bottom and other areas of the film are due to the evaporation of solvent and other volatile moieties. This is a commonly observed phenomenon in solution processed films. Fig.4a also shows a formation of a MoS_x layer at the Mo/CZTS interface during annealing. However, Raman and X-Ray diffraction spectra of the CZTS thin film do not display any characteristic peaks corresponding to MoS_x phase, which might be due to the very low thickness of the MoS_x layer. This also implies that a single phase CZTS film has been achieved within the absorption depth of the X-Ray and laser irradiation. In summary, modified annealing process has been found to have negligible impact on the reactivity of Mo with CZTS, but significantly reduces desorption of SnS and S_2 from film surface. From the cross sectional STEM image of the champion device shown in fig.4a, the thickness of MoS_x layer is 130 nm. Notably, other reports on high efficiency devices have also reported a similar thickness of this MoS_x layer in their devices.[4,22] The modified annealing process results in a slightly zinc rich composition of $Cu_{2.02\pm0.04}Zn_{1.28\ \pm0.03}SnS_{3.89\ \pm0.04}$ as determined by EDS (averaged from five random locations).

Solar cells with the standard device structure (total device area of 0.15 cm^2) were fabricated using the CZTS absorber layer obtained after annealing in 6% H_2S environment and modified annealing process. Fig.5 shows the current density-voltage (I-V) curve corresponding to the two solar cells under the AM 1.5 illumination. The photovoltaic performances of both the solar cells are summarized in Table 1. It can be observed that the efficiency of the solar cells containing CZTS thin film annealed in 6% H_2S gas, as shown in the first row of Table 1, yielded an efficiency of only 2.89%. This is significantly lower than anticipated, and is likely due to the non-homogeneous elemental composition in the absorber layer. We have observed a tremendous improvement in the efficiency with CZTS annealed under H_2S with externally supplied tin and sulfur environment. The corresponding I-V curve details obtained is also shown in the second row of Table 1. The measured efficiency of the champion device was 5.67%, with a 0.58V open circuit voltage which we believe is the highest of CZTS solar cell fabricated using sol-gel approach. In this modified annealing process with excess Sn and S environment, the current density, open circuit voltage and fill factor have all improved. Further, the I-V data of both CZTS solar cell devices as shown in Table 1 exhibit very low series resistance. We believe that the higher series resistance, compared with CIGS solar cells[30], observed here is partially due to the presence of thin MoS_x layer at Mo/CZTS interface. In addition, the shunt resistance of the champion device is also

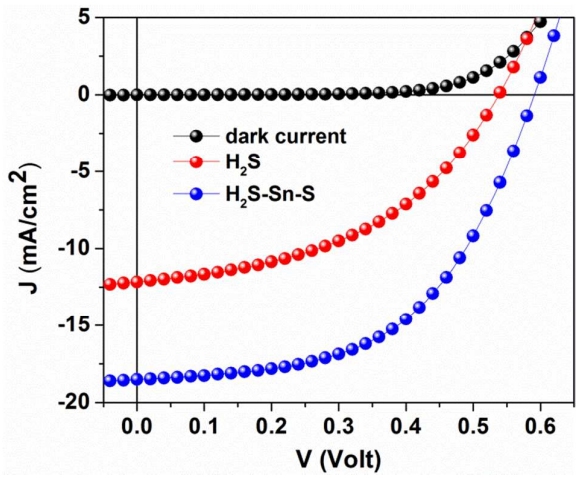

Fig.5 I-V characteristics of the champion solar cell devices under AM 1.5 illumination (i) CZTS annealed in 6% of H_2S environment, (ii) CZTS modified annealed in 6% of H_2S with externally provided Sn and Sulfur flakes. All devices are of 0.15 cm^2 area.

Table 1 Photovoltaic performance of CZTS annealed under 6% H_2S environment without and with externally supplied Sn and S environment

Annealed CZTS	η (%)	V_{OC} (Volt)	J_{SC} (mA/cm^2)	Fill Factor (%)	R_S (ohm.cm^2)
H_2S	2.89	0.53	12.11	45	3.75
H_2S-Sn-S	5.67	0.58	18.48	53.14	3.37

lower, which causes low fill factor, than what is generally reported for these types of devices.[31] From the EDS line scan, it can be clearly observed that Cu has migrated through the MoS_x layer at the CZTS/Mo interface, which is the probable cause of leakage for the observed the observed low V_{OC} and FF.[32]

In order to investigate if electrical and optical losses originating from other layers in the champion device, photoresponse of the champion CZTS device was determined using external quantum efficiency (EQE) measurement as shown in fig.6a. The observed electrical loss in the short wavelength region (below 500 nm) is due to the absorption in the buffer and window layers, while the electrical loss observed in the longer wavelength (600 to 850 nm) region is may be due to incomplete absorption in CZTS or recombination losses. The band gap of the CZTS layer is determined to be 1.52 eV by fitting a plot of $[E\ln(1\text{-}EQE)]^2$ vs. E near the band edge, as shown in the Fig.6b. This is in good agreement with the band gap determined from the optical absorption spectrum of the absorber layer as shown in the fig.S4 of the supporting information.

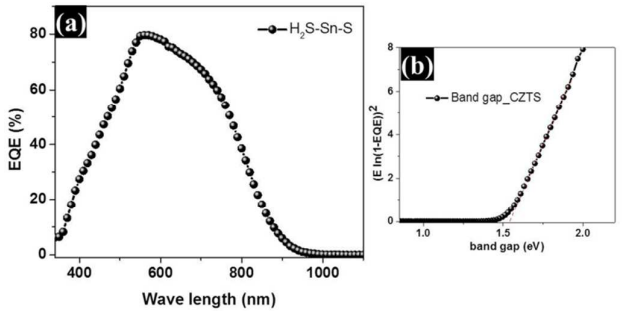

Fig.6 a) External Quantum Efficiency (EQE) spectrum of the champion device, b) band gap of CZTS deduced from the EQE spectrum.

Semi empirical calculations[33] show that the reduction in thicknesses of buffer and window layers can improve the charge collection in the short wavelength region due to the reduced absorption in these layers. In order to achieve this, the CZTS thin film quality in terms of homogeneity of composition through thickness must be very high and also the thin film surface must be very smooth. Otherwise, reduction in thicknesses of buffer and window layers may result non-homogeneous or partial deposition on CZTS absorber and may yields low conversion efficiencies. In the tube furnace annealing process, the cooling after annealing may lead to different growth profiles of CZTS thin film. Therefore, further optimization of the cooling rates via rapid thermal annealing process may suppress the SnS and S_2 desorption even further and likely result in even better quality of the CZTS film. Further enhancement in the device efficiency can be achieved if the series resistance is reduced by means of reducing the thickness of MoS_x layer.

Conclusions

We have reported here successful synthesis of homogeneous CZTS precursor ink by introducing a non-toxic solvent, DMI, by sonication at room temperature. A thorough investigation was conducted in order to understand the properties of CZTS at high temperatures to grow a high quality CZTS thin-film. These investigations included optimization of sol-gel concentration, annealing temperature, annealing time and H_2S concentration. The effect of H_2S concentration during annealing process on the grain size was optimized, and it is found that at 6% of H_2S concentration, pore-free CZTS thin film with large grain size and Mo/CZTS interface free of carbon-rich layer or small grains was yielded. Additionally, in the modified annealing process, externally supplied tin and sulfur environment during the annealing significantly improved the suppression of desorption of SnS and S_2 from the CZTS surface, resulting in a homogenous composition of the CZTS film. In this work, the champion device fabricated with the standard structure has achieved a record high efficiency of 5.67%.
The conclusions section should come in this section at the end of the article, before the acknowledgements.

Acknowledgements

We thank the Ministry of Science and Technology (MOST), Academia Sinica, Taiwan International Graduate Program (TIGP), National Taiwan University, National Tsing-Hua University and Ministry of Education (MOE), Taiwan for financial support. We also would like to thank Ministry of Science and Technology (National Taiwan University) FIB operator, Ms.Chia-Ying Chien for the assistance in preparing the TEM sample. Technical support from Nano-Core, the core facilities for nanoscience and nanotechnology at Academia Sinica in Taiwan, is acknowledged.

Notes and references

1 B. A. Andersson, Prog Photovolt Res Appl., 2000, **8**, 61-76.
2 M. Graetzel, R. A. Janssen, D. B. Mitzi and E. H. Sargent, *Nature*, 2012, **488**, 304-312.
3 T. Gokmen, O. Gunawan, T. K. Todorov and D. B. Mitzi, *Appl Phys Lett.,* 2013, **103**, 103506-103510.
4 W. Wang, M. T. Winkler, O. Gunawan, T. Gokmen, T. K. Todorov, Y. Zhu and D. B. Mitzi, *Adv Energy Mater.*, 2014, **4**, 1301465-1301469.
5 M. A. Green, K. Emery, Y. Hishikawa, W. Warta and E. D. Dunlop, *Prog Photovolt Res Appl.,* 2013, **21**, 827-837.
6 T. K. Todorov, K. B. Reuter and D. B. Mitzi, *Adv Mater.*, 2010, **22**, E156-159.
7 J. Kim, H. Hiroi, T. K. Todorov, O. Gunawan, M. Kuwahara, T. Gokmen, D. Nair, M. Hopstaken, B. Shin, Y. S. Lee, W. Wang, H. Sugimoto and D. B. Mitzi, Adv Mater, 2014, **26**, 7427-7431.

8 K. Woo, Y. Kim and J. Moon, Energ Environ Sci., 2012, **5**, 5340-5345.
9 J. W. Cho, A. Ismail, S. J. Park, W. Kim, S. Yoon and B. K. Min, *ACS Appl Mater Interfaces*, 2013, **5**, 4162-4165.
10 K. Tanaka, N. Moritake and H. Uchiki, *Sol Energ Mat Sol C*, 2007, **91**, 1199-1201.
11 W. Yang, H. S. Duan, B. Bob, H. Zhou, B. Lei, C. H. Chung, S. H. Li, W. W. Hou and Y. Yang, *Adv Mater.*, 2012, **24**, 6323-6329.
12 C. M. Fella, A. R. Uhl, Y. E. Romanyuk and A. N. Tiwari, *physica status solidi (a)*, 2012, **209**, 1043-1048.
13 G. M. Ilari, C. M. Fella, C. Ziegler, A. R. Uhl, Y. E. Romanyuk and A. N. Tiwari, *Sol Energ Mat Sol C*, 2012, **104**, 125-130.
14 G. Wang, W. Zhao, Y. Cui, Q. Tian, S. Gao, L. Huang and D. Pan, *ACS Appl Mater Interfaces*, 2013, **5**, 10042-10047.
15 Z. Su, K. Sun, Z. Han, H. Cui, F. Liu, Y. Lai, J. Li, X. Hao, Y. Liu and M. A. Green, *J Mater Chem A*, 2014, **2**, 500-509.
16 T. K. Chaudhuri and D. Tiwari, *Sol Energ Mat Sol C*, 2012, **101**, 46-50.
17 J. B. Li, V. Chawla and B. M. Clemens, *Adv Mater.*, 2012, **24**, 720-723.
18 K. Maeda, K. Tanaka, Y. Nakano, Y. Fukui and H. Uchiki, *Jpn J Appl Phys.*, 2011, **50**, 05FB09.
19 K. Maeda, K. Tanaka, Y. Fukui and H. Uchiki, Sol Energ Mat Sol C, 2011, **95**, 2855-2860.
20 J. J. Scragg, J. T. Watjen, M. Edoff, T. Ericson, T. Kubart and C. Platzer-Bjorkman, J Am Chem Soc., 2012, 134, 19330-19333.
21 O. Gunawan, T. K. Todorov and D. B. Mitzi, Appl Phys Lett., 2010, **97**, 233506-233508.
22 B. Shin, O. Gunawan, Y. Zhu, N. A. Bojarczuk, S. J. Chey and S. Guha, *Prog Photovolt Res Appl.,* 2013, **21**, 72-76.
23 J. J.Scragg, Copper Zinc Tin Sulfide Thin films for Photovoltaics, illustrated edn., Springer Science & Business Media, 2011.
24 J. J. Scragg, T. Ericson, X. Fontané, V. Izquierdo-Roca, A. Pérez-Rodríguez, T. Kubart, M. Edoff and C. Platzer-Björkman, Prog Photovolt Res Appl., 2014, **22**, 10-17.
25 J. van Embden, A. S. Chesman, E. Della Gaspera, N. W. Duffy, S. E. Watkins and J. J. Jasieniak, J Am Chem Soc., 2014, **136**, 5237-5240.
26 Y. Cao, M. S. Denny, Jr., J. V. Caspar, W. E. Farneth, Q. Guo, A. S. Ionkin, L. K. Johnson, M. Lu, I. Malajovich, D. Radu, H. D. Rosenfeld, K. R. Choudhury and W. Wu, J Am Chem Soc., 2012, **134**, 15644-15647.
27 A. Weber, R. Mainz and H. W. Schock, J Appl Phys., 2010, **107**, 013516-013521.
28 J. J. Scragg, T. Ericson, T. Kubart, M. Edoff and C. Platzer-Bjorkman, Chem Mater., 2011, **23**, 4625-4633.
29 A. Redinger, D. M. Berg, P. J. Dale and S. Siebentritt, J Am Chem Soc, 2011, **133**, 3320-3323.
30 D. A. R. Barkhouse, O. Gunawan, T. Gokmen, T. K. Todorov and D. B. Mitzi, Progress in Photovoltaics: Research and Applications, 2012, **20**, 6-11.
31 K. Wang, O. Gunawan, T. Todorov, B. Shin, S. J. Chey, N. A. Bojarczuk, D. Mitzi and S. Guha, Appl Phys Lett, 2010, **97**, 143508-143510.
32 K. Wang, B. Shin, K. B. Reuter, T. Todorov, D. B. Mitzi and S. Guha, Appl Phys Lett., 2011, **98**, 051912-051914.
33 M. T. Winkler, W. Wang, O. Gunawan, H. J. Hovel, T. K. Todorov and D. B. Mitzi, Energ Environ Sci., 2014, **7**, 1029-1036.

Table of contents:

We are introducing a non-toxic solvent, 1,3-dimethyl-2-Imadazolidinone, for the preparation of CZTS ink and demonstrated 5.67% efficiency CZTS device.